Nano Energy 69 (2020) 104417

Contents lists available at ScienceDirect

Nano Energy

journal homepage: http://www.elsevier.com/locate/nanoen

Nestable arched triboelectric nanogenerator for large deflection biomechanical sensing and energy harvesting

Jingwen Liao [a,b], Yang Zou [b], Dongjie Jiang [b], Zezhi Liu [d], Xuecheng Qu [b], Zhe Li [b], Ruping Liu [d], Yubo Fan [c], Bojing Shi [c,**], Zhou Li [b,***], Li Zheng [a,*]

[a] College of Mathematics and Physics, Shanghai Key Laboratory of Materials Protection and Advanced Materials in Electric Power, Shanghai University of Electric Power, Shanghai, 200090, China

[b] CAS Center for Excellence in Nanoscience, Beijing Key Laboratory of Micro-Nano Energy and Sensor, Beijing Institute of Nanoenergy and Nanosystems, Chinese Academy of Sciences, Beijing, 100083, China

[c] Beijing Advanced Innovation Centre for Biomedical Engineering, Key Laboratory for Biomechanics and Mechanobiology of Ministry of Education, School of Biological Science and Medical Engineering, Beihang University, Beijing, 100083, China

[d] Beijing Institute of Graphic Communication, Beijing, 102600, China

ARTICLE INFO

Keywords:
Triboelectric nanogenerator
Biomechanical sensing
Wearable
Nestable
Large angle deflection

ABSTRACT

Flexible and wearable electronics has presented an opportunity to evolve our society into an intelligent world. Especially for biomechanical sensing and gesture recognition, wearable devices are quite indispensable. Here, we present a nestable arched triboelectric nanogenerator (NA-TENG), which can be wore on fingers, acting as a large deflection biomechanical sensor and energy harvester. With arched structure, the sensor can detect large bending angle of fingers with good stability. Meanwhile, the NA-TENG devices can be assembled like matryoshka, which greatly increases the extensibility for optimizing output performance of the NA-TENG, and provides a convenient method to regulate characteristics of TENG devices in wearable applications.

1. Introduction

Modern electronics, which are irreplaceable for human health, safety and communication, present a wide spectrum of opportunities to evolve our society into an intelligent world [1–3]. To this end, flexible and wearable electronics has attracted considerable attention owing to their promising applications in a wide range of fields, ranging from flexible power supply [4–6], stretchable circuits [7–9], personal healthcare/biomedical monitoring [10–12], artificial electronic skin [13–15] to wearable human-interactive interface.

However, the application of wearable electronics still faces several critical challenges. First, for the recording of electrical signals from the body, the operations of these wearable electronics usually require external power sources which have rigid circuit boards that are heavy and have bulky volume, with limited capacity and lifetime [16–18]. Second, conventional planar structure may be degraded or even damaged due to the large deformations of the human body motions that may destroy the structure and function of wearable electronics [19–21]. Third, low detection limit and the maximum detection strain are the key indicators for a biomechanical sensor. With these disadvantages, the practical and sustainable use of wearable electronic devices is largely hindered [22–24]. Developing new devices and methods are necessary to achieve low detection limit and high stability which plays an important role in expanding the working strain range [25–27].

Recently, massive efforts have been devoted to developing flexible stretchable sensor with combined characteristics of flexibility, broad sensing range, high sensitivity, and mechanical stability [28–30]. With these unremitting efforts, many types of self-powered functional sensors for health monitoring [31–33], motion tracking [34], medical care, personal protection, and security have been developed. These wearable sensor systems with ultra-thinness, soft robotics, low modulus [35–37], light weight, high flexibility, and stretchability [38,39], which can contact with the surface of the skin or the organs conformally, could provide an exciting opportunity for a continuous, real-time human--activity monitoring and personal healthcare [40–42]. This kind of self-powered sensors are usually based on triboelectric nanogenerator

* Corresponding author.
** Corresponding author.
*** Corresponding author.
E-mail addresses: bjshi@buaa.edu.cn (B. Shi), zli@binn.cas.cn (Z. Li), zhengli@shiep.edu.cn (L. Zheng).

https://doi.org/10.1016/j.nanoen.2019.104417
Received 25 October 2019; Received in revised form 17 December 2019; Accepted 19 December 2019
Available online 23 December 2019

(TENG) which rely on the electrostatic induction and triboelectrification [43–45]. With TENG, the mechanical energy can be converted into electricity by triboelectrification and electrostatic induction. It has been demonstrated that it is capable to harvest different types of ubiquitous energies so that TENG solves the problem that electronics need to contact with extra power sources which are heavy and cumbersome [46, 47]. Nowadays, there are some designs that are three dimensional (3D) and arch-structured based on TENG. Thanks to these structures, the sensors can be applied to some curved parts of the human body. When the human body moves, the sensors can be deformed conformally without damaging the structure and its function. In addition, a series of materials, including carbon black, carbon nanotube (CNT), graphene and metallic nanowire have been widely incorporated into flexible polymer matrices to prepare biomechanical sensors [48–50].

In this work, we design a nestable arched triboelectric nanogenerator (NA-TENG) that can be bent with large angle to act as large deflection biomechanical sensor. The NA-TENG consists of two silicone rubber arch layers is single-electrode TENG, where one has aluminum (Al) film on the silicone rubber layer while the other is just silicone rubber. With layers increasing, the operation mode of the device will change, the outputs will be enhanced up and some interesting phenomenon appear. The NA-TENG can be assembled like matryoshka, which can not only optimize the outputs but also provide an interesting approach to design new style of TENG devices.

2. Results and discussion

Silicone rubber is one of the most common materials for fabricating flexible sensor which processes multiple characteristics such as low Young's modulus, superior elasticity, stretchability and good physical and chemical stability in the air. As a matter of fact, after two different materials come into contact with each other, a chemical bond is formed between the two surfaces and charges move from one material to the other to equalize the electrostatic potential between them. To screen the induced potential difference, the transferred charges will drive free electrons to flow back and forth in circuit. As Fig. 1a shows, the silicone rubber acts as both flexible substrate and friction layer, while an Al film attached to the silicone rubber is used as both electrode and another friction layer of the NA-TENG. When the device is in bending state, the device will be bent to make the rubber and Al film contact and separate, thus the applied mechanical energy is converted into electricity. As mentioned before, the NA-TENG can detect large bending angles. The silicone and Al film will be contacted completely when the arch is deformed to a certain degree. When the bending state is recovering, the two layers begin separate. As a result, free electrons in the ground will flow into the aluminum electrode to balance the electrostatic potential. Due to the electrostatic induction, positive charges are induced in the bottom silicone rubber layer which generates an instantaneous current. When the two friction layers separate absolutely, both the amount of transferred charges and the electrical potential of the Al electrode reach their maximum values, reaching a state of electrical equilibrium. When the top silicone rubber becomes in contact with the aluminum film again, a reverse instantaneous current is generated. As a result, the periodic contact-separation process between silicone rubber and Al film will generate instantaneous alternating potential and current through the load.

The output of two NA-TENG devices are characterized separately under a linear motor with the same frequency, same motion speed of the contact-separation and same pressure between the two contacting films. To imitate the index finger bending movement, one edge of the device is fixed to a stage, the other edge is hung up which would contact and separate with linear motor to deform the arch of device (Fig. 2a). The output of open-circuit voltage (V_{OC}), transferred charge (Q_{TR}) and short-circuit current (I_{SC}) of the two devices are presented in Fig. 2b–d. To make it clear, we named the two devices as No.1 and No.2 with the out-layer radii of 5 mm and 6 mm, respectively. The peak value of the V_{OC} of the No.1 and No.2 devices are 2.4 V and 2.7 V, respectively. The corresponding peak values of the Q_{TR} of them are 0.7 nC and 1.2 nC, respectively, while the peak values of I_{SC} of the No.1 and No.2 devices

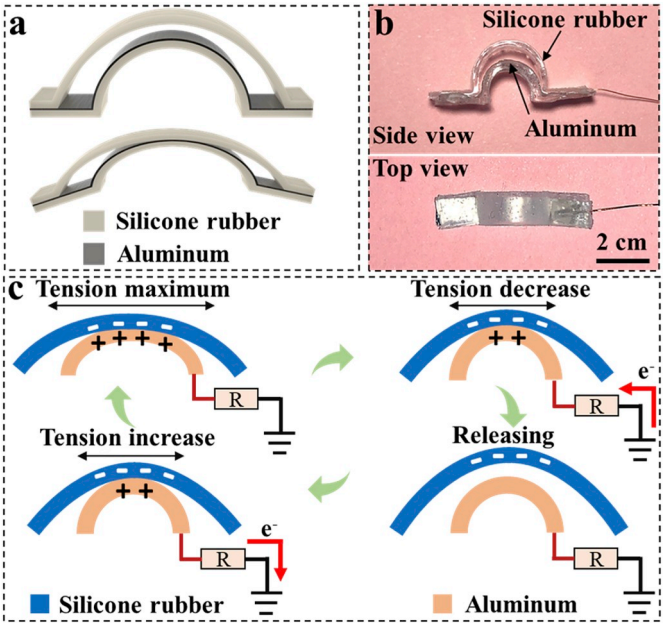

Fig. 1. (a) Diagram of NA-TENG at original and bending states. (b) Photos of NA-TENG from side and top views. (c) Working principle of NA-TENG when actuated by external tension.

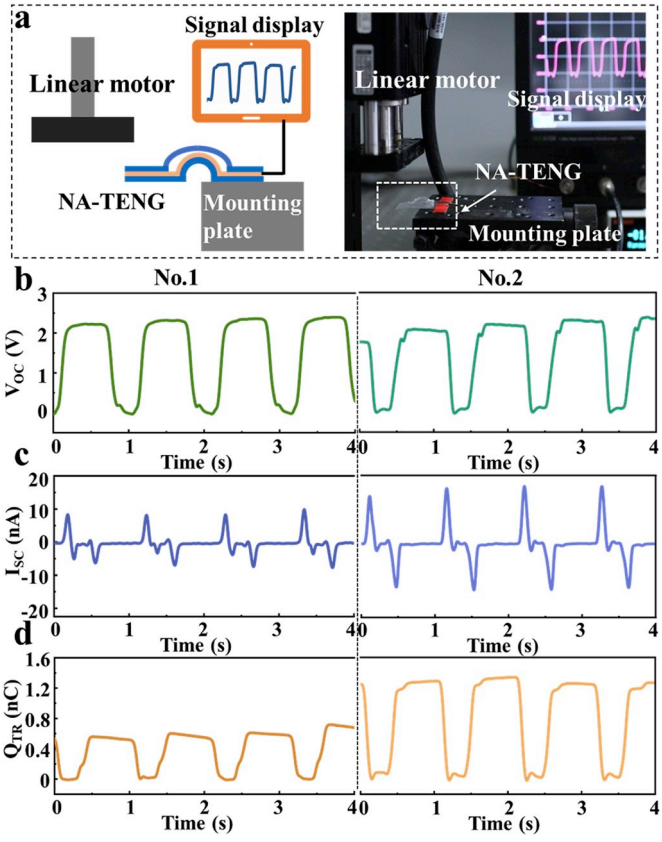

Fig. 2. (a) Diagram and Photo of NA-TENG bent by linear motor. (b) Open-circuit voltages of the two devices. (c) Short-circuit currents of the two devices. (d) Transferred charges of the two devices.

are ~10 nA and ~15 nA, respectively. Due to different gap depth of the arches, the outputs of device No.2 is higher than that of No.1.

Due to the characteristics of large angle that the device could be bent, we apply the NA-TENG to detect the movements of knuckles (Fig. 3a and b). We fabricate the device with top silicone layer with semicircle radius of 5 mm and bottom silicone layer with semicircular radius of 3 mm and apply it to the fingers to characterize the bending output. The relationship between the bending angles of the finger and the corresponding outputs of the NA-TENG is shown in Fig. S1. It is obvious that the electrical outputs of this device increase with the increase of bending angles, showing its feasibility for being used in recognition of different gestures. As the index finger repeats the actions of bending and straightening slowly, the real-time output voltage shows a gradual and periodic synchronous increasing and decreasing, showing a real-time

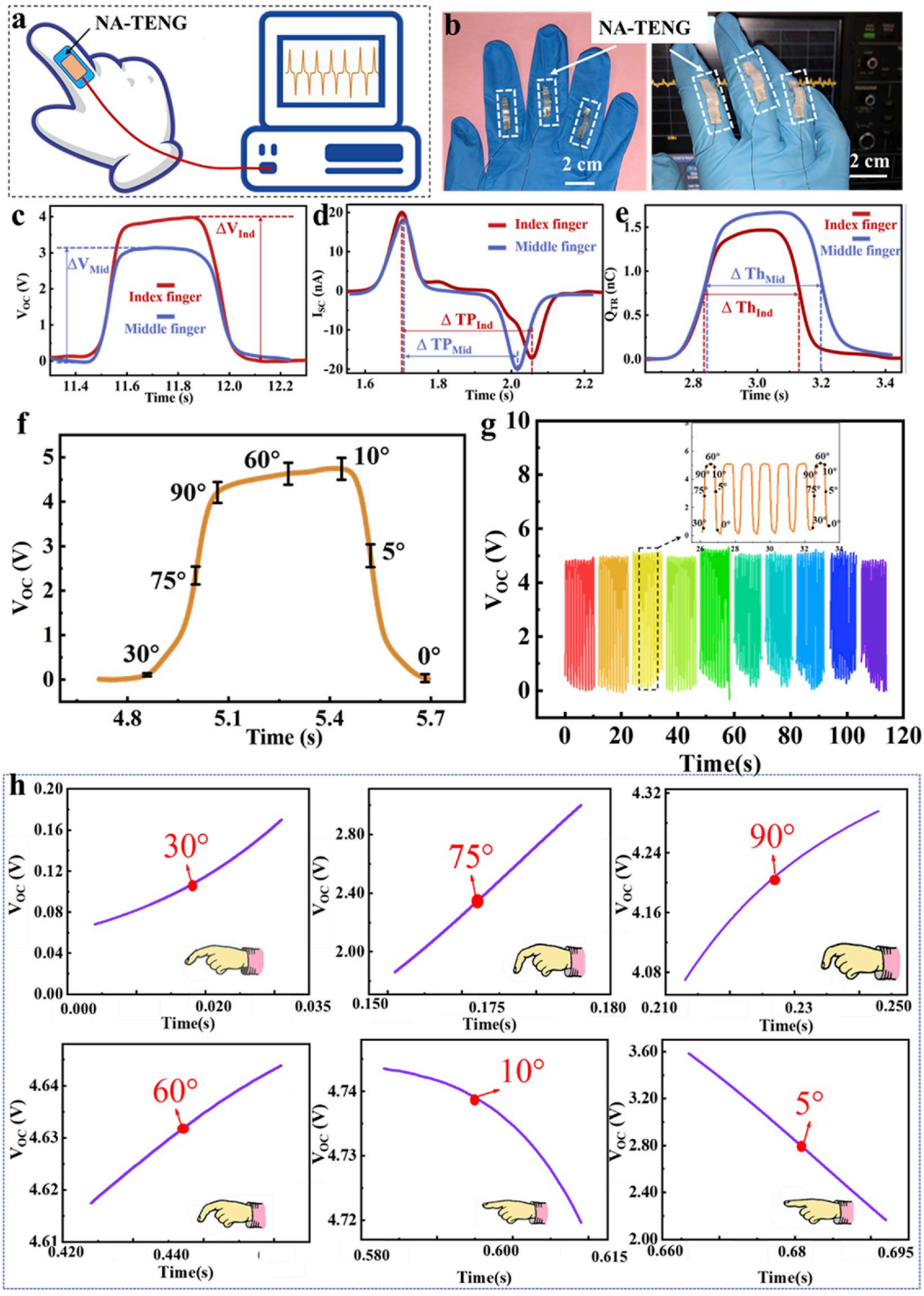

Fig. 3. (a) Diagram of NA-TENG applied on finger. (b) Photos of NA-TENG applied on fingers. (c) Comparison of open-circuit voltages of NA-TENGs applied on index and middle figures. (d) Comparison of short-circuit currents of NA-TENGs applied on index and middle figures. (e) Comparison of transferred charges of NA-TENGs applied on index and middle figures. (f) Relationship of bending degrees of finger with output of NA-TENG (g) Repeatable test of NT-TENG by bending fingers 200 cycles. (h) Details of relationship of bending degrees of finger with output of NA-TENG.

self-powered finger motion detection. In the same time, because of the superior structure of the device, the NA-TENG could detect a sharp angle of the finger. The outputs detected by bending the finger are showed in Figs. S2 and S3. The peak value of the V_{oc} is ~4 V and that of the Q_{TR} is ~1.5 nC. Under short-circuit conditions, the peak value of measured I_{sc} is ~20 nA. A control group experiment in which added saline is shown in Fig. S4. It is obvious that the output voltage of the saline group decreases because the single electrode.

Fig. 3c–e shows the data of index finger and middle finger, respectively. By contrast, it is found that some parameters extracted from these

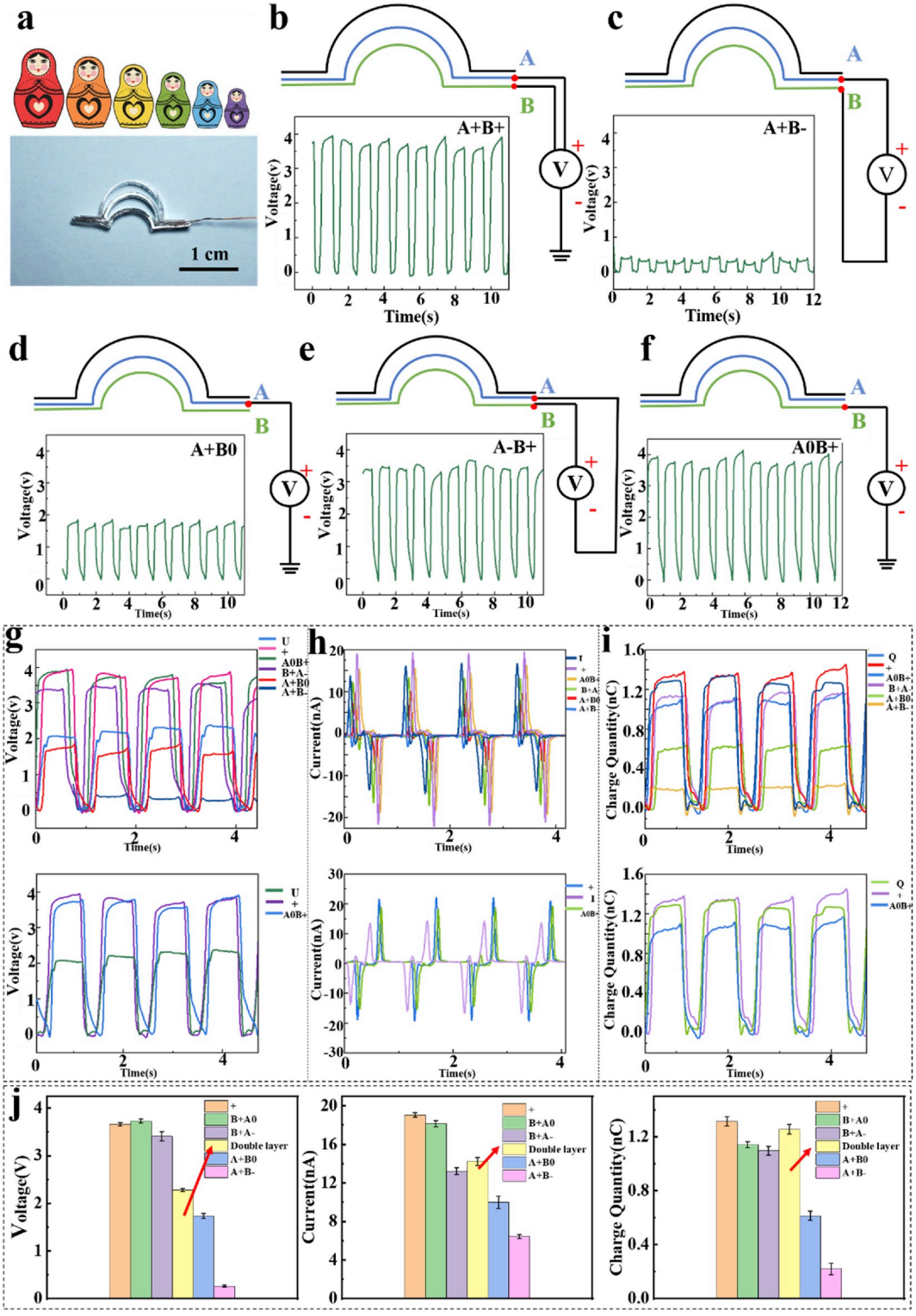

Fig. 4. (a) Nested NA-TENG inspired by matryoshka. (b–f) Open-circuit voltages of nested NA-TENG under different conditions of wire connection. (g) Comparison of open-circuit voltages of nested NA-TENG under different conditions of wire connection. (h) Comparison of short-circuit currents of nested NA-TENG under different conditions of wire connection. (i) Comparison of transferred charge quantities of nested NA-TENG under different conditions of wire connection. (j) Comparison of peak values of outputs of nested NA-TENG under different conditions of wire connection.

data can be used to reflect the difference of devices activated by different fingers, such as voltage difference (ΔV), time interval between peak and trough of wave (ΔTP) and full width at half maxima (ΔTh). The NA-TENG can realize a real-time monitoring of bending finger movement by analyzing the electrical signals from the arched device.

The electrical signals corresponding to multiple bending actions of the fingers statistically is also analyzed, and the results is shown in Fig. 3f–h. It is found that some prominent angles of the signals corresponding to the finger bending movement, which are 30°, 75°, 90°, 60°, 10°, 5°, 0°, respectively. The angle of 30° represents a start of a bending movement, and the point of 75° represents the middle point during the ascend of the electrical signal. At the point of 90°, the finger bends to the maximum angle. At the process of 30°–90°, the electrical output increases sharply. The next is the recovering process during the unbending of finger. When the finger recovering to the point of 60°, the electrical output still increase slowly that may be due to the hysteresis effect of triboelectrification [35]. The electrical output reaches the maximum value when the bending finger recovers to the point of 10°. It is clearly shown that the bending degree of finger changes sharply during the period from 90° to 10°, but the electrical output changes gently. We speculate that the two friction layers contact entirely when the finger recover to 10° so that the output reaches to a peak value. In the next process of the point of 10°–0°, the electrical output enters the decay period. When the finger recovers entirely, the electrical output also approaches to zero infinitely. As shown in Fig. 3f, the sensitive and accurate NA-TENG can convert the bending movement of finger to the electrical signal as a biomechanical angle sensor which can be used in real-time angle monitoring. The results of repeatable test by bending fingers (200 times) are showed in Fig. 3g. There is no significance attenuation of the outputs and the electrical signals corresponding to multiple bending actions of the fingers are stable. The results of the contract area for some prominent angles of the signals corresponding to the finger bending movement are showed in Fig. S5. Thanks to its highly sensitivity and accuracy, the NA-TENG can also be used as gesture sensor to detect different gestures.

To study the relation between the sensing properties and the size of NA-TENG, a smaller device with a size of 5 mm × 10 mm is fabricated. The electrical outputs detected by bending the finger are demonstrated in Fig. S6. The peak value of voltage is ~1.7 V and that of charge quantity is ~0.4 nC. Under short-circuit conditions, the peak value of measured current is ~0.4 nA. It is demonstrated that the output of smaller NA-TENG is lower than before. We also test the voltage of a control group experiment in which added saline and the result. It is obvious that the output voltage of the saline group decreases. To further optimize the electrification materials, we modified the arched layer by incorporating polymer materials into the silicone rubber. The outputs of the modified devices are shown in Fig. S7. The results showed that the outputs of the $BaTiO_3$ nanoparticles (NPs) mixed NA-TENG have a most significant improvement, followed by carbon nanotubes and PVDF powders mixed devices.

Here, we propose a minimalist design of a three layers device based on matryoshka as shown in Fig. 4a. The matryoshka device has three layers, in which bottom and middle layers are made of same materials-silicone rubber and Al film but sizes are different. The bottom and middle layer film is in semicircle shape with radius of 3 mm and 5 mm, respectively, while the top layer of the matryoshka with semicircle radius of 7 mm. As the matryoshka device stack layer by layer, the operation mode of the device changes. The matryoshka can be more than three layers, and with increasing of layers, some interesting phenomenon appears. Here, we just discuss the device with three layers. According to the two wires of the device, we design five connection methods, shown in Fig. 4b–f. Here, we call the middle wire as A and the bottom wire as B.

The first connection way is that both A and B connect with the positive electrode of the electrometer while the negative electrode connects with the ground. The second connection way is that A connects with the positive electrode while B connects with the negative electrode. The third connection way is that A connects with the positive electrode while the negative electrode connects with the ground. The fourth connection way is that A connects with the negative electrode while B connects with the positive electrode. And the last connection method is that B connects with the positive electrode while the negative electrode connects with the ground. The five connection methods can be divided into five groups to compare the difference of the outputs. To compare the output data from different connection way, the first connection way is grouped as No.1 and the second and fourth connection ways are grouped as No.2. The No.3 group contains the third and last connection ways. The No.4 group contains the second and third connection ways. The No.5 group contains the fourth and last connection ways.

We measure V_{oc}, Q_{TR}, I_{sc} of the matryoshka in each connection way, we analyze the data, then select group No.1, the device of two layers and the matryoshka device with the last connection way together for further analysis. Compared all these electrical outputs, the data of each peak value of the V_{oc}, Q_{TR}, I_{sc} of five connection ways and the device of two layers are analyzed and shown in Fig. 4j. From the comparison of No.2 and No.3 group, there is a phenomenon that the output is higher when B connect with the positive electrode than A connect with the positive electrode. And from the comparison of No.4 and No.5 group, the output of the matryoshka device when the negative electrode connects with the ground is higher than that of the device when it connects with A or B. When analyzing the No.1 group, it is obvious that the output that both A and B connect with the positive electrode is the highest, compared with other connection methods. Here are some hypothesis. In the matryoshka device, it mainly relies on the bottom layer to generate electricity. When the negative electrode connects with the ground, a part of the matryoshka is similar to a single-electrode TENG. Therefore, when the negative electrode connects with the ground, the output will be more stable. There is an interesting phenomenon that the largest peak value of V_{oc} is the matryoshka device of No.1 group, which is almost twice as much as the output of the device with two layers. And the peak value of I_{sc} of the matryoshka device with this connection method is higher than the device with two layers. As for the Q_{TR}, there is no big difference between the matryoshka device in the first connection method and the device with two layers. We suspect that the matryoshka device may become a capacitor. According to the following capacitor formulas, $Q = \int Idt$, $Q = \varepsilon \frac{SU}{d}$, because the charge quantity of No.1 has no big difference with the device of two layers, and the current of No.1 is higher than the device with two layers so that the time of No.1 group must be shorter than that of the device with two layers. As a matter of fact, there is a time delay in the output peak from the device with two layers, shown in the Supporting Information Fig. S2d. As for the voltage, the peak value of V_{oc} of No.1 is higher than the device with two layers, so the distance of No.1 group must be longer than the device with two layers. In fact, the distance from the top layer to the bottom layer of the matryoshka device is longer than the device with two layers. In this project, we only discuss three layers based on matryoshka and we find out that the outputs increase with the increase of layers. When layers increasing, there will be more interesting phenomenon. It is thought-provoking and worth to be investigated.

To further show the scalability of the NA-TENG in wearable electronics, a nested NA-TENG with large triple layer is fabricated for energy harvesting, which can be wore on the wrist (Fig. 5a). Larger size means higher output. We use the nested NA-TENG bent by linear motor with frequency of 2 Hz to light LED bulbs and charge a capacitor (Fig. 5b). The output properties of the nested NA-TENG are tested by the linear motor with frequencies of 1 Hz, 2 Hz and 3 Hz, respectively (Fig. 5c–e). The results show that the outputs of the nested NA-TENG are higher than that of the previous double layered one and smaller triple layered one. To make the device smaller and more ingenious, we used different materials and fabrication methods to fabricate another miniaturized triple layered NA-TENG. (Fig. S8). PET (Polyethylene terephthalate) is

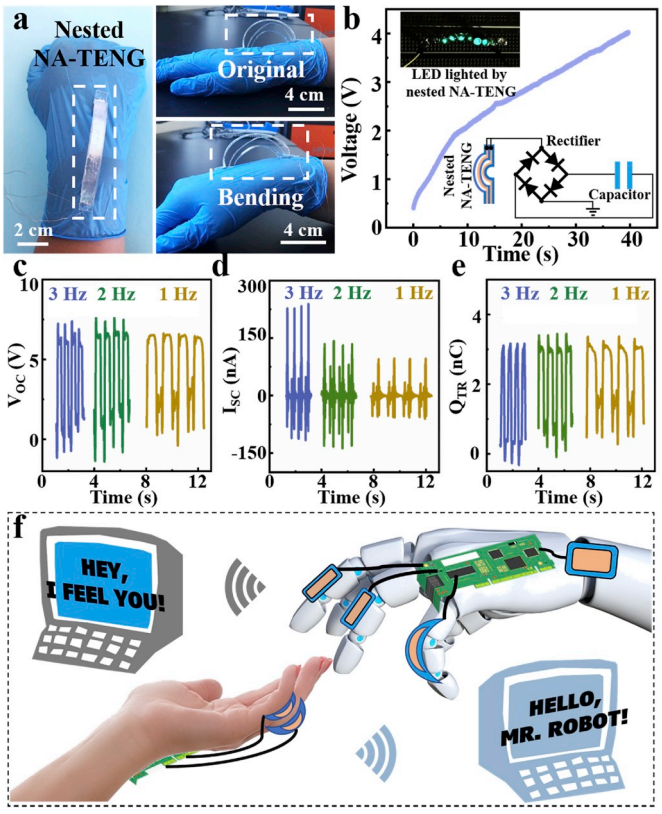

Fig. 5. (a) Photos of nested NA-TENG applied in elbow. (b) Charging curve of a 0.47 μF capacitor charged by nested NA-TENG. (Inset: six LED bulbs lighted by nested NA-TENG directly) (c) Open-circuit voltage of nested NA-TENG bent by linear motor with under different frequencies (1 Hz, 2 Hz, 3 Hz). (d) Short-circuit current of nested NA-TENG bent by linear motor with under different frequencies (1 Hz, 2 Hz, 3 Hz). (e) Transferred charges of nested NA-TENG bent by linear motor under different frequencies (1 Hz, 2 Hz, 3 Hz). (f) Schematic illustration of deploying NA-TENG in the wearable sensors and robot hand.

introduced to make the arched structure of the device through thermoforming process. The thickness of each layer is 100 μm. The length of the main part of the triple layered device is about 3 mm and the height is about 2 mm. Meanwhile, the Al foil electrode is replaced by a thin Al electrode deposited by magneton sputtering. Based on the ingesting characteristics of the NA-TENG, we anticipate the future wearable electronics and robots based on the NA-TENG and related designs in Fig. 5f. Various ingenious gesture sensors can be fabricated to be wore on hands and integrated in robotic arms more conveniently.

3. Conclusion

In summary, a nestable arched triboelectric nanogenerator with the advantages of highly flexible, stable and reliable features, is designed and fabricated for real-time large deflection angle sensor. Two different NA-TENG devices are fabricated and characterized, showing that with the longer the distance of the two layers, the higher of the output will be. The NA-TENG is applied to fingers to detect the bending angles. By analyzing the relationship between the electrical signal and the angles of bending finger, it is obvious that the NA-TENG is sensitive as an angle sensor which can be bent in a very large deflection angle. Moreover, the NA-TENG based on matryoshka can be assembled, and here we only fabricate a device with three layers and find that the electrical outputs increase with the increase of layers. It is the most important meaning of the matryoshka NA-TENG that it could provide an interesting approach to design new style of TENGs.

4. Experimental section

4.1. Fabrications of NA-TENG

First, we mixed Ecoflex 00–10 AB glue in a 1:1 ratio and then we put the mixture into a tailored mode. The length of whole device is 2 cm when the width is 0.5 cm and the thickness is 1.5 mm. The radii of the inner and outer semicircles are 3 mm and 5 mm, respectively. We designed three different bending degree modes using as the top layer, the bottom layer of the NA-TENG and the matryoshka's top layer. The NA-TENG's top layer and bottom layer are in semicircle shape with a radius of 5 mm and 3 mm, respectively. And the top layer of matryoshka is also in semicircle shape with radius of 7 mm. The middle and bottom layer of matryoshka are the top and bottom layer of NA-TENG. And then, we put the modes into the oven at 80 °C for half an hour. Stripped the cured silicone from the mold. The size of aluminum film is based on the size of NA-TENG's top and bottom silicone layer. The aluminum film was bonded with the NA-TENG's bottom layer using silicone glue and then connected with wires. The bottom and top layer were bonded together in a same way. The NA-TENG fabrication is completed. The fabrication method of the matryoshka is as same as the NA-TENG. When combined the NA-TENG with fingers, we need to find out the proximal interphalangeal (PIP) joint of finger, and then align the semicircular tip of the device with the PIP joint.

Three polymer materials were incorporated into silicone rubber to modify the layer of NA-TENG. Barium titanate ($BaTiO_3$) nanoparticles (Aladdin, particle size $<$ 100 nm), multi-walled carbon nanotubes (Shenzhen Nanotech Port Co. Ltd, range of diameter 10–20 nm) and poly (vinylidene fluoride) (PVDF) powders (SIGMA-ALDRICH, average Mw $\sim$ 534000) were mixed with the preformed gel of Ecoflex 00–10 with a mass ratio of 7.5% respectively and stirred well. Then three mixtures were poured into a PTFE mold and evacuated in a vacuum drying box, cured at 60 °C for 2 h and removed from the PTFE mold.

4.2. Characterizations of NA-TENG

The signal of NA-TENG is measured by the electrometer (Keithley 6517B). The sampling rate is 5 ks/s when the electrical signal is characterized. The linear motor is used to make the device work. One edge of the NA-TENG is fixed into a stable stage, and the other edge is suspended to connect and separate with the linear motor. The output of the device when we bended the index finger's PIP joint are recorded by the electrometer.

Acknowledgements

This study was supported by the National Key R&D project from Minister of Science and Technology, China (2016YFA0202703, 2016YFC1102202), National Natural Science Foundation of China (61875015, 31571006, 81601629, 11421202 and 21801019), the Beijing Natural Science Foundation (2182091), Research and Development Program of BIGC (Ec201808), the Beijing Municipal Science and Technology Commission (Z181100004418004), Science and Technology Commission of Shanghai Municipality (No.17020501000), the Program for Professor of Special Appointment (Eastern Scholar) at Shanghai Institutions of Higher Learning, the Ministry of Education of China (TP2017076) and the National Youth Talent Support Program.

Appendix A. Supplementary data

Supplementary data to this article can be found online at https://doi.org/10.1016/j.nanoen.2019.104417.

References

[1] K. Dong, J. Deng, W. Ding, A.C. Wang, P. Wang, C. Cheng, Y.C. Wang, L. Jin, B. Gu, B. Sun, Z.L. Wang, Versatile core–sheath yarn for sustainable biomechanical energy harvesting and real-time human-interactive sensing, Adv. Energy Mater. 8 (2018) 1–12, https://doi.org/10.1002/aenm.201801114.

[2] T. He, Z. Sun, Q. Shi, M. Zhu, D.V. Anaya, M. Xu, T. Chen, M.R. Yuce, A.V.Y. Thean, C. Lee, Self-powered glove-based intuitive interface for diversified control applications in real/cyber space, Nano Energy 58 (2019) 641–651, https://doi.org/10.1016/j.nanoen.2019.01.091.

[3] T.Q. Trung, N.E. Lee, Flexible and stretchable physical sensor integrated platforms for wearable human-activity monitoringand personal healthcare, Adv. Mater. 28 (2016) 4338–4372, https://doi.org/10.1002/adma.201504244.

[4] C. Dagdeviren, Z. Li, Z.L. Wang, Energy harvesting from the animal/human body for self-powered electronics, Annu. Rev. Biomed. Eng. 19 (2017) 85–108, https://doi.org/10.1146/annurev-bioeng-071516-044517.

[5] S. Kim, J. Han, M.A. Kang, W. Song, S. Myung, S.W. Kim, S.S. Lee, J. Lim, K.S. An, Flexible chemical sensors based on hybrid layer consisting of molybdenum disulphide nanosheets and carbon nanotubes, Carbon N. Y. 129 (2018) 607–612, https://doi.org/10.1016/j.carbon.2017.12.065.

[6] X. Cao, Y. Jie, N. Wang, Z.L. Wang, Triboelectric nanogenerators driven self-powered electrochemical processes for energy and environmental science, Adv. Energy Mater. 6 (2016), https://doi.org/10.1002/aenm.201600665.

[7] X. Chen, Y. Song, Z. Su, H. Chen, X. Cheng, J. Zhang, M. Han, H. Zhang, Flexible fiber-based hybrid nanogenerator for biomechanical energy harvesting and physiological monitoring, Nano Energy 38 (2017) 43–50, https://doi.org/10.1016/j.nanoen.2017.05.047.

[8] F. Yi, J. Wang, X. Wang, S. Niu, S. Li, Q. Liao, Y. Xu, Z. You, Y. Zhang, Z.L. Wang, Stretchable and waterproof self-charging power system for harvesting energy from diverse deformation and powering wearable electronics, ACS Nano 10 (2016) 6519–6525, https://doi.org/10.1021/acsnano.6b03007.

[9] Y. Jie, X. Jia, J. Zou, Y. Chen, N. Wang, Z.L. Wang, X. Cao, Natural leaf made triboelectric nanogenerator for harvesting environmental mechanical energy, Adv. Energy Mater. 8 (2018) 1–7, https://doi.org/10.1002/aenm.201703133.

[10] F. Yi, L. Lin, S. Niu, J. Yang, W. Wu, S. Wang, Q. Liao, Y. Zhang, Z.L. Wang, Self-powered trajectory, velocity, and acceleration tracking of a moving object/body using a triboelectric sensor, Adv. Funct. Mater. 24 (2014) 7488–7494, https://doi.org/10.1002/adfm.201402703.

[11] H. Ouyang, J. Tian, G. Sun, Y. Zou, Z. Liu, H. Li, L. Zhao, B. Shi, Y. Fan, Y. Fan, Z. L. Wang, Z. Li, Self-powered pulse sensor for antidiastole of cardiovascular disease, Adv. Mater. 29 (2017) 1–10, https://doi.org/10.1002/adma.201703456.

[12] Y. Zou, P. Tan, B. Shi, H. Ouyang, D. Jiang, Z. Liu, H. Li, M. Yu, C. Wang, X. Qu, L. Zhao, Y. Fan, Z.L. Wang, Z. Li, A bionic stretchable nanogenerator for underwater sensing and energy harvesting, Nat. Commun. 10 (2019) 1–10, https://doi.org/10.1038/s41467-019-10433-4.

[13] C. Zhu, A. Chortos, Y. Wang, R. Pfattner, T. Lei, A.C. Hinckley, I. Pochorovski, X. Yan, J.W.F. To, J.Y. Oh, J.B.H. Tok, Z. Bao, B. Murmann, Stretchable temperature-sensing circuits with strain suppression based on carbon nanotube transistors, Nat. Electron. 1 (2018) 183–190, https://doi.org/10.1038/s41928-018-0041-0.

[14] P.K. Yang, L. Lin, F. Yi, X. Li, K.C. Pradel, Y. Zi, C.I. Wu, J.H. He, Y. Zhang, Z. L. Wang, A flexible, stretchable and shape-adaptive approach for versatile energy conversion and self-powered biomedical monitoring, Adv. Mater. 27 (2015) 3817–3824, https://doi.org/10.1002/adma.201500652.

[15] Y. Jie, Q. Jiang, Y. Zhang, N. Wang, X. Cao, A structural bionic design: from electric organs to systematic triboelectric generators, Nano Energy 27 (2016) 554–560, https://doi.org/10.1016/j.nanoen.2016.07.028.

[16] J. Xu, S. Wang, G.N. Wang, C. Zhu, S. Luo, L. Jin, X. Gu, S. Chen, V.R. Feig, J.W. F. To, S. Rondeau-gagné, J. Park, B.C. Schroeder, C. Lu, J.Y. Oh, Y. Wang, Y. Kim, H. Yan, R. Sinclair, D. Zhou, G. Xue, B. Murmann, C. Linder, W. Cai, J.B. Tok, Highly stretchable polymer semiconductor films through the nanoconfinement effect, Res. Rep. 64 (2017) 59–64, https://doi.org/10.1126/science.aah4496.

[17] Z. Liu, Y. Ma, H. Ouyang, B. Shi, N. Li, D. Jiang, F. Xie, D. Qu, Y. Zou, Y. Huang, H. Li, C. Zhao, P. Tan, M. Yu, Y. Fan, H. Zhang, Z.L. Wang, Z. Li, Transcatheter self-powered ultrasensitive endocardial pressure sensor, Adv. Funct. Mater. 29 (2019) 1–10, https://doi.org/10.1002/adfm.201807560.

[18] H. Feng, C. Zhao, P. Tan, R. Liu, X. Chen, Z. Li, Nanogenerator for biomedical applications, Adv. Healthc. Mater. 7 (2018) 1–18, https://doi.org/10.1002/adhm.201701298.

[19] C. Wang, K. Hu, W. Li, H. Wang, H. Li, Y. Zou, C. Zhao, Z. Li, M. Yu, P. Tan, Z. Li, Wearable wire-shaped symmetric supercapacitors based on activated carbon-coated graphite fibers, ACS Appl. Mater. Interfaces 10 (2018) 34302–34310, https://doi.org/10.1021/acsami.8b12279.

[20] C. Baek, J.H. Yun, J.E. Wang, C.K. Jeong, K.J. Lee, K. Il Park, D.K. Kim, A flexible energy harvester based on a lead-free and piezoelectric BCTZ nanoparticle-polymer composite, Nanoscale 8 (2016) 17632–17638, https://doi.org/10.1039/c6nr05784e.

[21] J. Koo, M.R. MacEwan, S.K. Kang, S.M. Won, M. Stephen, P. Gamble, Z. Xie, Y. Yan, Y.Y. Chen, J. Shin, N. Birenbaum, S. Chung, S.B. Kim, J. Khalifeh, D.V. Harburg, K. Bean, M. Paskett, J. Kim, Z.S. Zohny, S.M. Lee, R. Zhang, K. Luo, B. Ji, A. Banks, H.M. Lee, Y. Huang, W.Z. Ray, J.A. Rogers, Wireless bioresorbable electronic system enables sustained nonpharmacological neuroregenerative therapy, Nat. Med. 24 (2018) 1830–1836, https://doi.org/10.1038/s41591-018-0196-2.

[22] X. Pu, M. Liu, X. Chen, J. Sun, C. Du, Y. Zhang, J. Zhai, W. Hu, Z.L. Wang, Ultrastretchable, transparent triboelectric nanogenerator as electronic skin for biomechanical energy harvesting and tactile sensing, Sci. Adv. 3 (2017) 1–11, https://doi.org/10.1126/sciadv.1700015.

[23] M.H. Seo, J.Y. Yoo, S.Y. Choi, J.S. Lee, K.W. Choi, C.K. Jeong, K.J. Lee, J.B. Yoon, Versatile transfer of an ultralong and seamless nanowire array crystallized at high temperature for use in high-performance flexible devices, ACS Nano 11 (2017) 1520–1529, https://doi.org/10.1021/acsnano.6b06842.

[24] L. Lonini, A. Dai, N. Shawen, T. Simuni, C. Poon, L. Shimanovich, M. Daeschler, R. Ghaffari, J.A. Rogers, A. Jayaraman, Wearable sensors for Parkinson's disease: which data are worth collecting for training symptom detection models, Npj Digit. Med. 1 (2018), https://doi.org/10.1038/s41746-018-0071-z.

[25] B. Shi, Z. Li, Y. Fan, Implantable energy-harvesting devices, Adv. Mater. 30 (2018) 1–18, https://doi.org/10.1002/adma.201801511.

[26] Y. Chu, J. Zhong, H. Liu, Y. Ma, N. Liu, Y. Song, J. Liang, Z. Shao, Y. Sun, Y. Dong, X. Wang, L. Lin, Human pulse diagnosis for medical assessments using a wearable piezoelectret sensing system, Adv. Funct. Mater. 28 (2018) 1–10, https://doi.org/10.1002/adfm.201803413.

[27] X. Chen, Q. Xu, S. Bai, Y. Qin, A self-powered sensor with super-hydrophobic nanostructure surfaces for synchronous detection and electricity generation, Nano Energy 33 (2017) 288–292, https://doi.org/10.1016/j.nanoen.2017.01.023.

[28] J. Sun, X. Pu, M. Liu, A. Yu, C. Du, J. Zhai, W. Hu, Z.L. Wang, Self-healable, stretchable, transparent triboelectric nanogenerators as soft power sources, ACS Nano 12 (2018) 6147–6155, https://doi.org/10.1021/acsnano.8b02479.

[29] Y. Wu, Q. Zeng, Q. Tang, W. Liu, G. Liu, Y. Zhang, J. Wu, C. Hu, X. Wang, A teeterboard-like hybrid nanogenerator for efficient harvesting of low-frequency ocean wave energy, Nano Energy (2019) 104205, https://doi.org/10.1016/j.nanoen.2019.104205.

[30] K.H. Koh, Q. Shi, S. Cao, D. Ma, H.Y. Tan, Z. Guo, C. Lee, A self-powered 3D activity inertial sensor using hybrid sensing mechanisms, Nano Energy 56 (2019) 651–661, https://doi.org/10.1016/j.nanoen.2018.11.075.

[31] G. Liu, J. Chen, Q. Tang, L. Feng, H. Yang, J. Li, Y. Xi, X. Wang, C. Hu, Wireless electric energy transmission through various isolated solid media based on triboelectric nanogenerator, Adv. Energy Mater. 8 (2018) 1–7, https://doi.org/10.1002/aenm.201703086.

[32] Z. Li, H. Feng, Q. Zheng, H. Li, C. Zhao, H. Ouyang, S. Noreen, M. Yu, F. Su, R. Liu, L. Li, Z.L. Wang, Z. Li, Photothermally tunable biodegradation of implantable triboelectric nanogenerators for tissue repairing, Nano Energy 54 (2018) 390–399, https://doi.org/10.1016/j.nanoen.2018.10.020.

[33] X. Pu, H. Guo, J. Chen, X. Wang, Y. Xi, C. Hu, Z.L. Wang, Eye motion triggered self-powered mechnosensational communication system using triboelectric nanogenerator, Sci. Adv. 3 (2017) 1–8, https://doi.org/10.1126/sciadv.1700694.

[34] D.Y. Park, D.J. Joe, D.H. Kim, H. Park, J.H. Han, C.K. Jeong, H. Park, J.G. Park, B. Joung, K.J. Lee, Self-powered real-time arterial pulse monitoring using ultrathin epidermal piezoelectric sensors, Adv. Mater. 29 (2017) 1–9, https://doi.org/10.1002/adma.201702308.

[35] K. Meng, J. Chen, X. Li, Y. Wu, W. Fan, Z. Zhou, Q. He, X. Wang, X. Fan, Y. Zhang, J. Yang, Z.L. Wang, Flexible weaving constructed self-powered pressure sensor enabling continuous diagnosis of cardiovascular disease and measurement of cuffless blood pressure, Adv. Funct. Mater. 29 (2019) 1–10, https://doi.org/10.1002/adfm.201806388.

[36] T. Chen, Q. Shi, M. Zhu, T. He, L. Sun, L. Yang, C. Lee, Triboelectric self-powered wearable flexible patch as 3D motion control interface for robotic manipulator, ACS Nano 12 (2018) 11561–11571, https://doi.org/10.1021/acsnano.8b06747.

[37] L. Zheng, S. Dong, J. Nie, S. Li, Z. Ren, X. Ma, X.Y. Chen, H.X. Li, Z.L. Wang, Dual-stimulus smart actuator and robot-hand based on vapor-responsive PDMS film and triboelectric nanogenerator, ACS Appl. Mater. Interfaces 11 (2019) 42504–42511, https://doi.org/10.1021/acsami.9b15574.

[38] Y.C. Lai, J. Deng, S. Niu, W. Peng, C. Wu, R. Liu, Z. Wen, Z.L. Wang, Electric eel-skin-inspired mechanically durable and super-stretchable nanogenerator for deformable power source and fully autonomous conformable electronic-skin applications, Adv. Mater. 28 (2016) 10024–10032, https://doi.org/10.1002/adma.201603527.

[39] C.K. Jeong, J. Lee, S. Han, J. Ryu, G.T. Hwang, D.Y. Park, J.H. Park, S.S. Lee, M. Byun, S.H. Ko, K.J. Lee, A hyper-stretchable elastic-composite energy harvester, Adv. Mater. 27 (2015) 2866–2875, https://doi.org/10.1002/adma.201500367.

[40] S.P. Beeby, M.J. Tudor, N.M. White, Energy harvesting vibration sources for microsystems applications, Meas. Sci. Technol. 17 (2006), https://doi.org/10.1088/0957-0233/17/12/R01.

[41] L. Lu, Y. Zhou, J. Pan, T. Chen, Y. Hu, G. Zheng, K. Dai, C. Liu, C. Shen, X. Sun, H. Peng, Design of helically double-leveled gaps for stretchable fiber strain sensor with ultralow detection limit, broad sensing range, and high repeatability, ACS Appl. Mater. Interfaces 11 (2019) 4345–4352, https://doi.org/10.1021/acsami.8b17666.

[42] Y. Mao, D. Geng, E. Liang, X. Wang, Single-electrode triboelectric nanogenerator for scavenging friction energy from rolling tires, Nano Energy 15 (2015) 227–234, https://doi.org/10.1016/j.nanoen.2015.04.026.

[43] Y. Zhang, W. Bai, X. Cheng, J. Ren, W. Weng, P. Chen, X. Fang, Z. Zhang, H. Peng, Y. Zhang, W. Bai, X. Cheng, J. Ren, W. Weng, P. Chen, X. Fang, Z. Zhang, H. Peng, Flexible and stretchable lithium-ion batteries and supercapacitors based on electrically conducting carbon nanotube fiber springs, Angew. Chem. Int. Ed. 53 (2014) 14564–14568, https://doi.org/10.1002/anie.201409366.

[44] Y.N. Guo, Z.Y. Gao, X.X. Wang, L. Sun, X. Yan, S.Y. Yan, Y.Z. Long, W.P. Han, A highly stretchable humidity sensor based on spandex covered yarns and nanostructured polyaniline, RSC Adv. 8 (2018) 1078–1082, https://doi.org/10.1039/c7ra10474j.

[45] L. Zheng, Y.L. Wu, X.Y. Chen, A. Yu, L. Xu, Y.S. Liu, H.X. Li, Z.L. Wang, Self-powered electrostatic actuation systems for manipulating the movement of both

microfluid and solid objects by using triboelectric nanogenerator, Adv. Funct. Mater. 27 (2017), https://doi.org/10.1002/adfm.201606408 adfm201606408.
[46] Y. Xie, S. Wang, S. Niu, L. Lin, Q. Jing, J. Yang, Z. Wu, Z.L. Wang, Grating-structured freestanding triboelectric-layer nanogenerator for harvesting mechanical energy at 85% total conversion efficiency, Adv. Mater. 26 (2014) 6599–6607, https://doi.org/10.1002/adma.201402428.
[47] C. Wang, C. Wang, Z. Huang, S. Xu, Materials and structures toward soft electronics, Adv. Mater. 30 (2018) 1–49, https://doi.org/10.1002/adma.201801368.
[48] B. Shi, Z. Liu, Q. Zheng, J. Meng, H. Ouyang, Y. Zou, D. Jiang, X. Qu, M. Yu, L. Zhao, Y. Fan, Z.L. Wang, Z. Li, Body-integrated self-powered system for wearable and implantable Applications, ACS Nano 13 (2019) 6017–6024, https://doi.org/10.1021/acsnano.9b02233.
[49] P. Tan, Q. Zheng, Y. Zou, B. Shi, D. Jiang, X. Qu, H. Ouyang, C. Zhao, Y. Cao, Y. Fan, Z.L. Wang, Z. Li, A battery-like self-charge universal module for motional energy harvest, Adv. Energy Mater. 1901875 (2019) 1901875, https://doi.org/10.1002/aenm.201901875.
[50] Z. Liu, H. Li, B. Shi, Y. Fan, Z.L. Wang, Z. Li, Wearable and implantable triboelectric nanogenerators, Adv. Funct. Mater. 29 (2019) 1–19, https://doi.org/10.1002/adfm.201808820.

Jingwen Liao received her B.S. degree from the North China University of Water Resources and Electric Power in 2017 and she is currently postgraduate at the Shanghai Institute of Electric Power. Her research direction is the application of triboelectric nanogenerators in biosystem.

Yang Zou received his B.S. degree in bioengineering from Beihang University in 2016. He is currently pursuing a Ph.D. degree in Nanoscience and Nanotechnology at the University of Chinese Academy of Sciences. His current research interests include soft energy harvesting devices and sensors, bionic electronics.

Dongjie Jiang received his bachelor's degree in Light Chemical Engineering (Excellence Program), Zhejiang Sci-Tech University in 2017. He is currently pursuing the Ph.D. degree in the Beijing Institute of Nanoenergy and Nanosystems, Chinese Academy of Sciences. His current interests include self-powered systems and applications based on nanogenerator.

Zezhi Liu is currently undergraduate at Beijing Institute of Graphic Communication. He has participated in the research of graphene oxide doped PVA soluble tape substrate. His current interests include triboelectric nanogenerator and self-powered sensors.

Xuecheng Qu received his B.S. degree in Electric Engineering and Automative from University of Jinan in 2017. He is currently pursuing the Ph.D degree with the Department of Biophysics, Beijing Institute of Nanoenergy and Nanosystems, Chinese Academy of Sciences. His current interests include self-powered sensors, systems and applications based on nanogenerators.

Zhe Li received the B.S. degree in college of science from Northeast Forestry University, Haerbin, China, in 2015. She is currently pursuing the Ph.D. degree in Beijing Institute of Nanoenergy and Nanosystems, Chinese Academy of Sciences. Her research work is focusing on the application of nanogenerator for self-powered biomedical systems, active sensors and energy storage device.

Ruping Liu received her B.S. degree in Materials Science from Wuhan University of Technology in 2002 and M.S. degree in Materials Science from Wuhan Research Institute of Materials Protection in 2006 and Doctor degree in Physical Electronics from Institute of Electronics, Chinese Academy of Sciences in 2010. She has been an associate professor of Beijing Institute of Graphic Communication (2013-). Her Current interests are flexible devices and sensing.

Yubo Fan is the Dean of School of Biological Science and Medical Engineering, Director of Key Laboratory for Biomechanics and Mechanobiology of Ministry of Education of Beihang University, Director of National Research Centre for Rehabilitation Technical Aids of China. He is the AIMBE Fellow, the President of Chinese Biomedical Engineering Society, Chair elect of World Association for Chinese Biomedical Engineers (WACBE), Vice president of China Strategic Alliance of Medical Devices Innovation, and Council Member of World Congress of Biomechanics. Prof. Fan specializes in bio-mechanics, mechanobiology, and biomaterials.

Bojing Shi received his Ph.D. from University of Chinese Academy of Sciences in 2017, and B.E. degree from University of Electronic Science and Technology of China in 2012. He is currently doing postdoctoral research at Beijing Advanced Innovation Centre for Biomedical Engineering, Beihang University. His research work is focusing on nanogenerators, implantable energy devices, and self-powered biosensors and systems.

Zhou Li, Ph.D., professor. He received his Ph.D. from Peking University in Department of Biomedical Engineering in 2010, and Medical Degree from Wuhan University in Medical School, 2004. He jointed School of Biological Science and Medical Engineering of Beihang University in 2010 as an associate Professor. Currently, he is a Professor in Beijing Institute of Nanoenergy and Nanosystems, CAS. His research interests include nanogenerators, in vivo energy harvester and self-powered medical devices, bio-sensors.

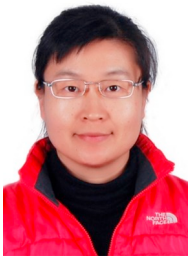

Li Zheng, Ph.D., professor. She received her Ph.D. from Shanghai Jiao Tong University in 2009. Currently, she is a Professor in Shanghai University of Electric Power. Her current research interests include nanogenerators and energy harvesting, nanostructure-based optoelectronic devices, and self-powered nanosystems.